OPTICAL REVIEW Vol. 17, No. 4 (2010) 379–384

Functional Imprinting Structures on GaN-Based Light-Emitting Diodes for Light Pattern Modulation and Light Extraction Efficiency Enhancement

Sheng-Han TU*, Shang-Yen WU, Yeeu-Chang LEE[1], Jui-Wen PAN[2], Cheng-Huang KUO, Chih-Ming WANG[3], and Jenq-Yang CHANG

Department of Optics and Photonics, National Central University, Jhongli, Taiwan 32001, R.O.C.
[1]*Department of Mechanical Engineering, Chung Yuan Christian University, Jhongli, Taiwan 32023, R.O.C.*
[2]*Institute of Photonic System, College of Photonics National Chiao Tung University at Tainan, Tainan County, Taiwan 71150, R.O.C.*
[3]*Institute of Opto-Electronic Engineering, National Dong Hwa University, Hualien, Taiwan 97401, R.O.C.*

(Received December 13, 2009; Accepted May 13, 2010)

In this study, we demonstrated a simple method that can be used to simultaneously modulate the far field pattern and enhance the light extraction of GaN-based light-emitting diodes (LEDs). In this method, microstructures were imprinted on a reliable spin-on-glass surface on top of a transparent conductive layer. The far-field pattern was modulated using microoptical structures, and at the same time, the light extraction was enhanced owing to the small refractive index difference and surface roughness. There was no decrease in the electrical performance of these devices. The peak intensity shifted from 0 to 22° in one-dimensional (1D) asymmetrically blazed periodic structures, and a flattened distribution with a uniform intensity within a span of 110° was observed in two-dimensional (2D) symmetrically periodic structures. This method achieved 13 and 40% light enhancements for 1D and 2D structures, respectively.

Keywords: GaN, light-emitting diode (LED), imprinting technology, far-field pattern modulation, light extraction

1. Introduction

GaN-based light-emitting diodes (LEDs) have attracted great interest owing to their small size, energy efficiency, longevity, and environmental soundness.[1–3] LEDs are used in many applications, including traffic lights, pocket-size projectors, plate panel displays, and so on.[4,5] However, there are still two restrictions for LED applications. First, the native Lambertian far-field pattern of an LED is not suitable for some applications.[6] Second, the light extraction of LED chips is only 4% owing to the Fresnel loss and total internal reflection (TIR) between air and the GaN interface.[7] In the Lambertian far-field case, additional optical elements, such as compound parabolic concentrators (CPCs)[8] and diffusers,[9] were used to modify the far-field pattern. Examples of this approach include a collimator light source for LED projectors[10] and a uniform intensity distribution for LED backlighting. Moreover, secondary optical structures can modify the far-field pattern of an LED. Micro- and submicrostructures were also fabricated on LED chips to achieve the same goal.[11,12]

In the case of light extraction enhancement, various methods, such as those considering surface roughness,[13] a patterned sapphire substrate (PSS)[14] and direct fabrication of micro- or submicrooptical structures on a p-GaN surface,[11,15] were adopted to improve light extraction. The imprinting process is one of several promising technologies for the mass production of micro/nanostructures. In 2007, Wang *et al.*[16] and Bao *et al.*[17] applied poly(dimethylsiloxane) (PDMS) and poly(methyl methacrylate) (PMMA) structures to LEDs using the imprinting technique. They demonstrated light extraction enhancement using embossed surface textures.

In this study, we demonstrated a simple method of imprinting one-dimensional (1D) and two-dimensional (2D) microoptical structures on a reliable spin-on-glass (SOG) surface. This method can be used to modulate the far-field pattern of an LED chip and enhance light extraction without decay in electric performance. The output light patterns exhibited a peak intensity shift in an angular distribution in 1D blazed grating structures and in a flattened distribution in 2D cylinder array structures. The proposed method achieved 13 and 40% light enhancements for 1D and 2D structures, respectively. These imprinted microoptical SOG structures offered the following three advantages for fabricating surface textures on LED transparent conductive layers (TCLs): light extraction enhancement, light pattern modulation, and LED light source size reduction.

2. Experimental Procedure

The native far-field pattern of LEDs was a Lambertian light source, as shown in Fig. 1(a).[18] A flat LED surface resulted in the peak intensity in the direction normal to the lighting surface and a half intensity at ±60° relative to the normal axis. In LEDs, light was produced by spontaneous emission from the active layer of the chip. Therefore, the light was incoherent and the lighting performance of the chip can be regarded as a linear superposition in intensity terms. In this study, we used the LED chip with a microstructure surface similar to that shown in Fig. 1(b). This chip consisted of a conventional LED with an additional layer of embossed SOG microstructures on top of a transparent conductive layer (TCL). In this device, the light emitted

*E-mail address: shdo1021@gmail.com

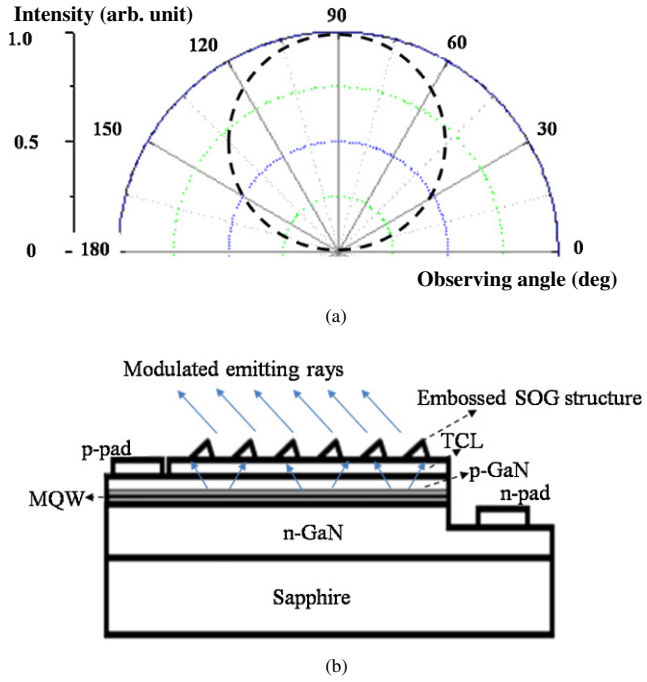

Fig. 1. (Color online) LED far-field pattern: (a) Lambertian far-field pattern of a native LED bare chip and (b) ray deflection in an expected direction by the embossed microstructure.

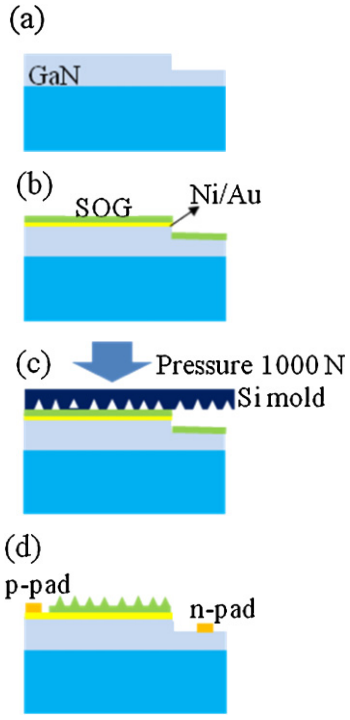

Fig. 2. (Color online) Flow chart of imprinted LED process: (a) LED mesa etching, (b) deposition of Ni/Au TCL and the spinning of SOG, (c) imprinting process with Si mold and 1000 N pressure, and (d) additional SOG removal and pad deposition.

from the active layer can be deflected to a specific direction with the designed microstructures. This design also enhanced the light extraction by the index difference reduction and interface roughness between air and the GaN interface.

The conventional unpackaged GaN-based LED chips used in this study were grown by metal organic chemical vapor deposition (MOCVD) with a peak emission wavelength of 460 nm. Figure 2 shows the imprinted LED process flow chart. In Fig. 2(a), the LED chip process, inductively coupled plasma (ICP) dry etching, was used to form a $300 \times 300\,\mu m^2$ mesa array of 500 nm height. After mesa etching, a TCL of Ni/Au (50 Å/100 Å) was deposited on the mesa using electron beam deposition. After TCL deposition, the SOG produced by Futurrex with serial number DC1200 was prepared for structure imprinting. Before the embossing process, the master molds were fabricated by traditional photolithography and anisotropic wet etching on Si chips. We spun the SOG on the TCL and soft-baked it to evaporate the solvent. After soft baking, the SOG thickness was 300 nm, as shown in Fig. 2(b). The sample was then embossed using the Si mold, as shown in Fig. 2(c). The imprinting process was completed with a 1000 Newton applied pressure for 2 min at room temperature. After separating the mold from the LED chip, the imprinted pattern was observed to be an identical copy of the master pattern, and the LED chip was then thermally annealed for SOG hardening. The property of hardened SOG was similar to that of silicon dioxide and the SOG exhibited stable and robust chemical and physical characteristics. The area of the mold ($0.5-1\,cm^2$) was slightly smaller than that of the LED sample ($1.5-2\,cm^2$). Although the SOG accumulated at the edges of the LED sample, the SOG accumulation did not affect the imprinting results significantly. The yield of the imprinted area was larger than 80%.

After the embossing process, the SOG covering the p- and n-pad areas was removed by high-density plasma (HDP) etching to allow further electrode deposition. The Cr/Au (500 Å/2500 Å) pad was coated onto the p- and n-GaN by electron beam deposition, as shown in Fig. 2(d). Finally, the LED was wire-bonding packaging for subsequent electrical and optical measurements.

The optical microscopy pictures of the imprinted structures after pad deposition are shown in Fig. 3. Figure 3(a) shows a picture of the SOG spun onto the LED chip surface after soft baking. Figure 3(a) shows that the SOG imprinted structure was distributed on the LED area flatly. There are two reasons for the flatness of the spun SOG on the LED mesa area. First, compared with the 300 µm mesa width, the trench width was only 40 µm. Second, the SOG thickness after soft baking was approximately 300 nm, which was smaller than the height of the mesa. Thus, most of the spun SOG covered the mesa area flatly. Only the SOG on the mesa area can contact the Si mold directly for pattern transferring. Figures 3(b) and 3(c) show the imprinted LED chips after pad deposition. Figures 3(b) and 3(c) show that both 1D blazed grating and 2D cylinder array structures were imprinted on the LED mesa area flatly and uniformly. In addition to the 1D blazed grating and 2D cylinder array structures, a conventional planar LED without the SOG layer was also prepared for comparison.

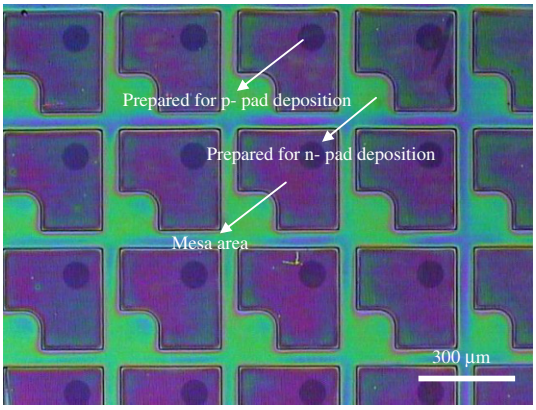

(a)

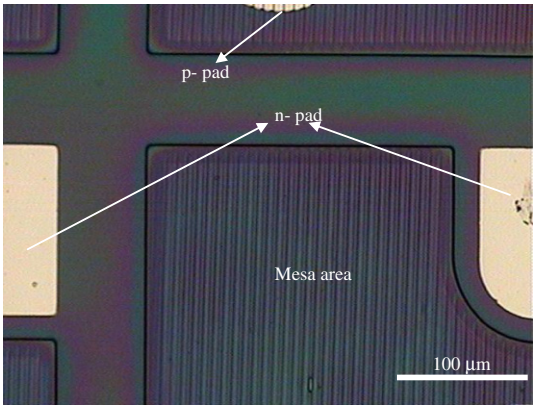

(b)

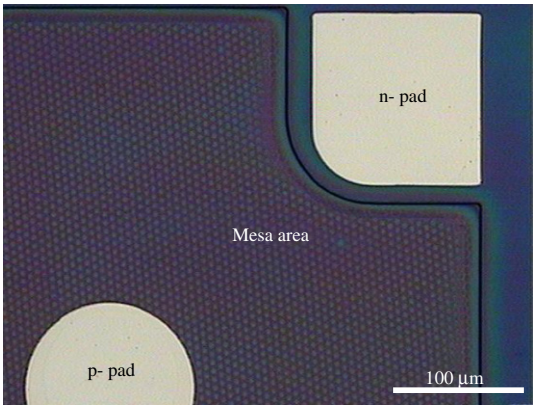

(c)

Fig. 3. (Color online) Optical microscopy pictures of the imprinting structures: (a) optical microscopy picture of SOG after soft baking, (b) optical microscopy picture of 1D blazed grating, and (c) optical microscopy picture of 2D cylinder array.

3. Results and Discussion

Figure 4 shows the atomic force microscopy (AFM) pictures and structure schemes of the 1D blazed grating and 2D cylinder array surfaces. Figure 4(a) shows the 1D blazed grating surface with a spatial asymmetrically blazed grating structure, while Fig. 4(b) shows its geometric parameters. The period of this grating structure was 6 μm with a filling factor 0.5, and its height was about 385 nm. The grating surface showed a serrated profile with an asymmetrically blazed structure, which had two different angles, 10 and 50°, between the sidewall and the bottom surface. This blazed structure can deflect light in the desired direction. Figure 4(c) indicates that the period and height of the 2D cylinder array structure were 5 μm and 260 nm, respectively, and its symmetrical sidewalls had an angle of 23°, as shown Fig. 4(d).

Figure 5(a) shows the injection current versus voltage (*I*–*V*) curves of planar, 1D blazed grating, and 2D cylinder array LEDs. The forward voltage of the planar LED was about 3.4 V, and the LEDs with 1D blazed grating and 2D cylinder array structures had similar electrical performance characteristics. Figure 5(b) shows the output power versus injection current (*L*–*I*) curves measured by integral sphere. The output power was enhanced by 13% for the 1D blazed grating LED and 40% for the 2D array structure LED, compared with that of the planar LED at an input current of 20 mA.

This output power enhancement was attributed to a reduction in the refractive index difference and the surface roughness. Although the escape light cone cannot be enlarged, the light emitted in normal propagation was enhanced by the insertion of SOG. The refractive index of SOG (1.5) resulted in a gradual reduction in the refractive index between air and the GaN interface. Thus, a reduction in the degree of light trapping resulting from Fresnel loss was achieved. The light output was also enhanced by the textured SOG surface layer. For the flat and orthogonal surfaces, when the light hit one surface and reflected to the other surface, the reflected light would be reflected by another surface. Thus, the light was trapped by a set of orthogonal closed surfaces. The GaN formed a trapping box that trapped light by its six orthogonal surfaces. However, after the insertion of the textured SOG film, the TIR of smooth and symmetric interfaces was destroyed. The imprinted structures afforded additional tilt surfaces for light escape. The light reflected by one surface could escape by hitting another tilt surface. Thus, more surfaces can afford more opportunities for light to escape. The 2D cylinder array structure had a higher light extraction efficiency than the 1D blazed grating structure because it had a higher side surface density.[19)]

The equipment used for far-field pattern measurement is shown in Fig. 6. The equipment included an LED chip holder, a photodetector, and a rotation stage. The LED chip was mounted on the chip holder and the photodetector was located in the normal direction of the LED chip. The distance between the LED chip holder and the photodetector was 30 cm. Both the 1D blazed grating and 2D cylinder array LED chips were measured at three different rotating angles Φ. The values of Φ were 0, 90, and 180°. The rotating stage rotated at the azimuth angle Ψ that varied from 0 to 180° with 1° intervals for spatial intensity distribution measurement.

Figure 7 shows the far-field pattern results of LEDs with a plain surface, a 1D blazed grating surface, and a 2D cylinder array surface. Instead of presenting all far-field pattern

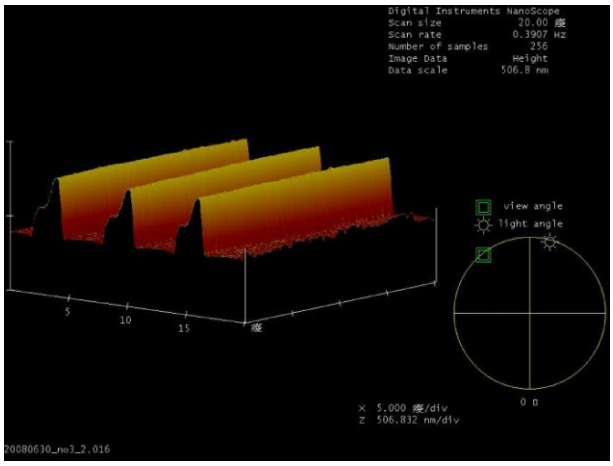

(a)

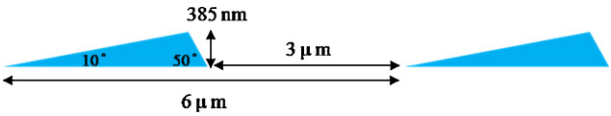

(b)

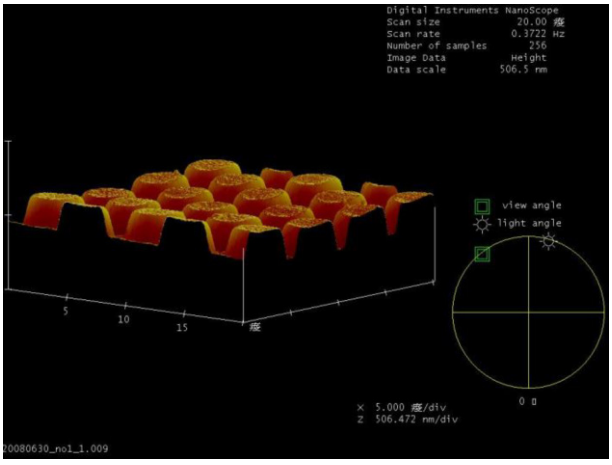

(c)

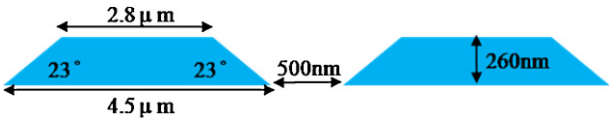

(d)

Fig. 4. (Color online) AFM images and geometric schemes of imprinted SOG structures: (a) AFM picture of 1D blazed grating structure, (b) 1D blazed grating geometric scheme, (c) AFM picture of 2D cylinder array structure, and (d) 2D cylinder array geometric scheme.

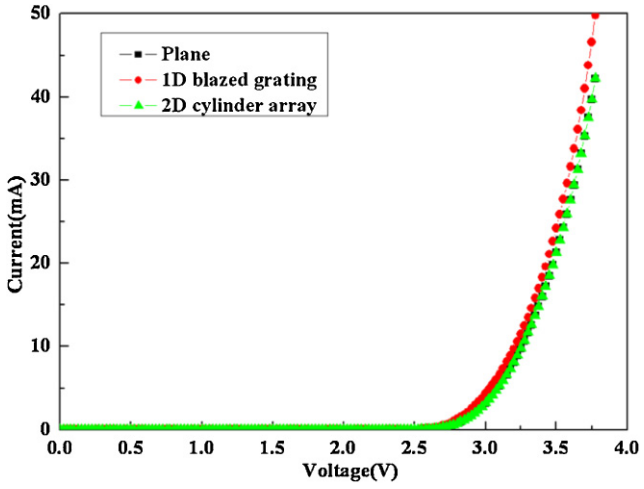

(a)

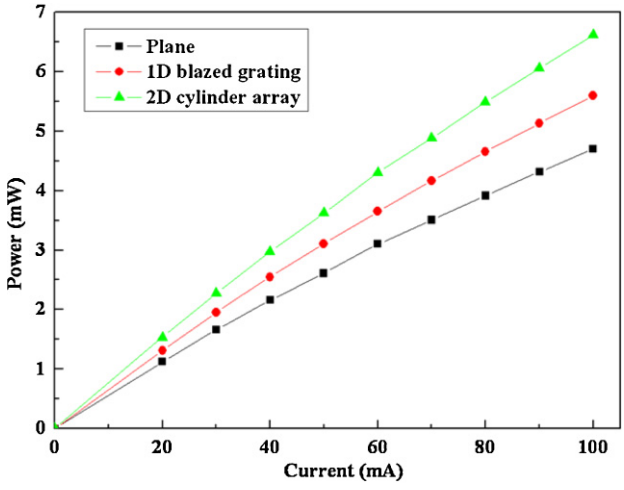

(b)

Fig. 5. (Color online) Electrical and optical performance characteristics of LEDs with and without imprinted structures: (a) output powers and (b) *I*–*V* curves of LEDs with and without embossed structure.

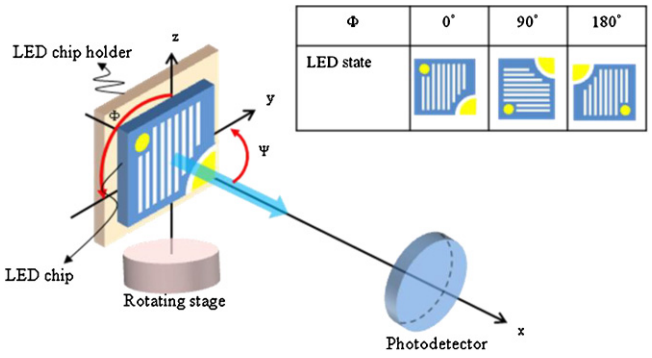

Fig. 6. (Color online) Equipment used for far-field pattern measurement.

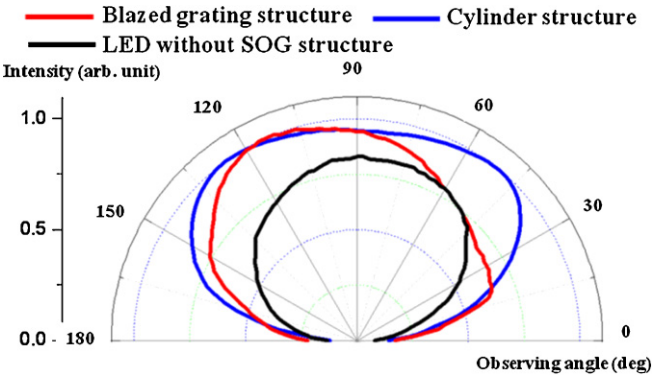

Fig. 7. (Color online) Far-field patterns of LEDs with embossed 1D blazed grating and 2D cylinder structures, and without the embossed structure.

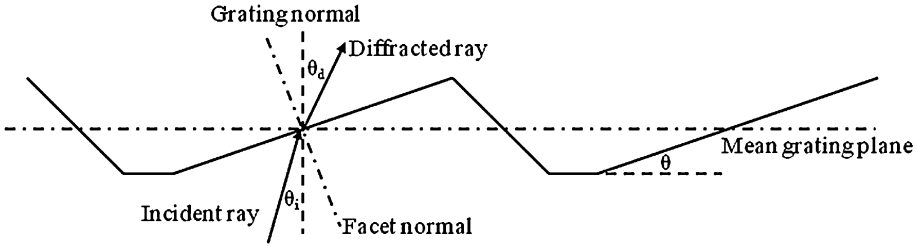

Fig. 8. Illustration of LED far-field pattern modulation resulting from 1D blazed grating.

results, Fig. 7 shows the basic differences among the measured results resulting from the imprinted structures. The plane LED had a Lambertian-like far-field pattern due to a native structure with a planar surface.[18] The peak intensity was deflected from the normal direction to 22° for the 1D blazed grating LED chip.

The half intensity angle of the 1D blazed grating LED chip was 150°. The half intensity angle of the planar LED chip was 136°. The half intensity angle span of the 1D blazed grating LED chip was similar to that of the planar LED chip. The far-field pattern intensity standard deviation (STD) inside the half-angle of the 1D blazed grating LED was 0.09, and the STD inside the half-angle of the planar LED was 0.1. The half-intensity angle span and the STD of intensity demonstrated that the 1D blazed grating provided a tilt and Lambertian-like far-field pattern of LEDs.

Figure 8 shows the relationship between the incident and diffracted rays through the blazed grating. The mean grating plane indicates the horizontal baseline of the blazed grating and the grating normal indicates the direction normalized to the mean grating plane. The angle between the incident ray and the grating normal was θ_i, while the angle between the grating normal and the diffracted ray was θ_d. The angle between the blazed grating facet and the mean grating plane was θ. Equation (1) shows the blazed grating theory obeyed by θ_i, θ_d, and θ:[20]

$$\theta = \frac{\theta_i - \theta_d}{2}. \quad (1)$$

For the native Lambertian property of LED chips, the peak intensity was incident in the grating normal direction; thus θ_i was 0° and θ was 10°. Using eq. (1), θ_d was determined to be 20°, which was consistent with the measured value of 22°.

The light source of an optical mouse was one example of the application of the tilted far-field pattern. Its optical module typically consists of an LED light source and an image system.[21] The current standard LED light source system consists of an LED positioned obliquely to a light-transferring element, and then, the LED light was transferred at an angle tilted toward the illuminated surface. The illuminated surface reflected light to the photodetector. However, the oblique assembly of the LED light source in an optical mouse restricts its alignment tolerance and flux utility.[21] LED chips with the angular asymmetry far-field patterns achieved using the 1D blazed grating structure can be assembled parallel to the surface illuminated with an oblique emitting light. This approach increases both alignment tolerance and flux utility.

Compared with the 1D blazed grating surface, the proposed 2D cylinder array produced a far-field pattern with a large full-width at half-maximum radiation angle of 160°. Figure 7 shows a uniform intensity distribution across an angle of 110°. At this uniform distribution angle, the intensity was more than 90% of the peak intensity, and the STD of the intensity distribution was only 0.018. In other words, the 2D cylinder array provided a uniform intensity distribution across a wide angle range.

Such a large uniform intensity distribution angle can be applied to an LED backlight system. In a flat panel display, an LED backlight system is used as an alternative to cold cathode fluorescent lamps (CCFLs) owing to its superior color presentation and power saving abilities. However, the native Lambertian far-field pattern of LED chips suffers from uneven color mixing and brightness distribution problems. To solve those problems, a large number of LEDs must be used. With the increasing number of LEDs, issues related to fabrication cost and thermal dissipation must be considered. Thus, a uniform intensity distribution across a large angle is a potential solution for LED backlight systems. The 2D cylinder array fabricated in this study provides a uniform intensity distribution that results in a uniform color mixing and brightness distribution without increasing the number of LEDs.[5)]

4. Conclusions

In this study, we demonstrated a combined imprinting and chip process technique to produce reliable SOG microoptical structures on LED chips. These structures simultaneously enhanced the output power and modulated the far-field patterns of GaN-based LEDs without introducing electrical performance decay. The output power enhancements were 13 and 40% for the 1D blazed grating and 2D cylinder array SOG-imprinted structures, respectively. The far-field patterns were also modified from Lambertian patterns to tilted and expanded formats. LED chips with these imprinted structures can markedly modulate the far-field patterns without the need for complex secondary optics in specific applications.

References

1) M. R. Krames, O. B. Shchekin, R. M. Mach, G. O. Muleller, L. Zhou, G. Harbers, and M. G. Craford: IEEE J. Disp. Technol. **3** (2007) 160.
2) T. Gessmann and E. F. Schubert: J. Appl. Phys. **95** (2004) 2203.
3) E. F. Schubert and J. K. Kin: Science **308** (2005) 1274.
4) G. Harbers, M. Keuper, and S. Paolini: Proc. IDW 03, 2003, p. 1585.
5) S. I. Chang, J. B. Yoon, H. Kim, J. J. Kim, B. K. Lee, and D. H. Shin: Opt. Lett. **31** (2006) 3016.
6) R. Joachim and W. Alexander: Proc. SPIE **6486** (2007) 64860Z.
7) A. David, T. Fuji, R. Sharma, K. McGroddy, S. Nakaruma, S. DenBarrss, E. L. Hu, C. Weisbuch, and H. Benisty: Appl. Phys. Lett. **88** (2006) 061124.
8) H. Murat, D. Cuypersa, and H. D. Smeta: Proc. SPIE **6196** (2006) 619604.
9) C. H. Chien and Z. P. Chen: Microsyst. Technol. **13** (2007) 1529.
10) S. H. Tu, J. W. Pan, C. M. Wang, Y. C. Lee, and J. Y. Chang: Opt. Rev. **16** (2009) 1.
11) K. McGroddy, A. David, E. Matioli, M. Iza, S. Nakaruma, S. DenBaars, J. S. Speck, C. Weisbuch, and E. L. Hu: Appl. Phys. Lett. **93** (2008) 103502.
12) H. Ichikawa and T. Baba: Appl. Phys. Lett. **84** (2004) 457.
13) T. Fuji, Y. Gao, R. Shrama, E. I. Hu, S. DenBaars, and S. Nakamura: Appl. Phys. Lett. **84** (2004) 855.
14) M. Khizar, Z. Y. Fan, K. H. Kim, J. Y. Lin, and H. X. Jiang: Appl. Phys. Lett. **86** (2005) 173504.
15) H. Ichikawa and T. Baba: Appl. Phys. Lett. **84** (2004) 457.
16) Z. M. Wang, X. J. Luo, S. Wang, C. X. Luo, M. H. Sun, K. Bao, B. Zhang, G. Y. Zhang, Y. G. Wang, Y. Chen, H. Ji, and Q. Ouyang: Semicond. Sci. Technol. **22** (2007) 279.
17) K. Bao, X. N. Kang, B. Zhang, T. Dai, C. Xiong, H. Ji, G. Y. Zhang, and Y. Chen: IEEE Photonics Technol. Lett. **19** (2007) 1840.
18) E. F. Schubert: *Light-Emitting Diodes* (Cambridge University Press, Cambridge, U.K., 2006) p. 94.
19) M. K. Lee, C. L. Ho, and P. C. Chen: IEEE Photonics Technol. Lett. **20** (2008) 252.
20) H. Ju, P. Zhang, J. Liang, S. Wang, and Y. Wu: J. Microlithogr. Microfabr. Microsyst. **4** (2005) 019701.
21) J. W. Pan, S. H. Tu, C. M. Wang, and J. Y. Chang: Appl. Opt. **47** (2008) 3406.